

# Bidirectional Reflectance of Organic Light-Emitting Displays

Aldo Badano, Shu-Jen Lee, Jerzy Kanicki, Edward F. Kelley and Robert J. Jennings

**Abstract**— The reflection properties of a display device influence the available contrast and affect the perception of low-luminance detail. We report on a Monte Carlo method for modeling the bidirectional reflectance of multi-layer structures used in thin-film organic light-emitting displays. The results show a predominant specular peak along with a quasi-Lambertian component and significant haze.

## I. INTRODUCTION

The effective physical contrast of display devices is affected by the achievable contrast generated by the light-producing or light-modulating elements, and by reflections of ambient light. In emissive displays that are typically highly reflective by design, the control of ambient light reflection is critical to achieve high contrast, especially when large luminance dynamic range is needed. For instance, in high-performance medical imaging cathode-ray tubes (CRTs), the glass faceplate is darkened to reduce diffuse reflections and is coated with an anti-reflection film to reduce the specular component. Previously, we studied the effect of display reflectance on the physical contrast in the low luminance end of the grayscale, and related human visual system performance to the maximum ambient illumination that maintains a perceptually linear luminance scale [1]. It has been shown that, for CRTs, the display reflectance can be characterized by the sum of two components: specular and diffuse reflections. However, in flat-panel displays, the complete description of reflectance is more complex and requires the evaluation of the bidirectional reflection distribution function (BRDF) [5, 11].

In this paper, we describe a computational method for modeling the BRDF of electronic displays that relies on an optical Monte Carlo simulation code developed to study light transport processes in emissive structures. We compute the angular emission distribution for a beam incident into devices having different structures. We present re-

sults for Lambertian and specular surfaces, for CRT monitors and for organic light-emitting displays (OLEDs).

## II. METHODS

### A. Monte Carlo simulations

The BRDF calculations are based on a Monte Carlo (MC) method developed for studying light transport effects in emissive structures [1]. The MC method makes use of the generation of photons with random directions according to a probability distribution function that describes the nature of the light source [3, 8]. In this analysis, the light source is a collimated beam or a collimated, distributed planar source, incident on the display surface with a direction determined by  $(\theta_i, \phi_i)$  with a given wavelength distribution  $S(\lambda)$ , and polarization state  $p$ . The photon histories are followed through a sequence of events that includes absorption, scattering and Fresnel refraction. The simulation models bulk absorption events, optically thin coatings and rough surfaces. The outcome of each individual event is dependent on the photon energy and polarization, and on the material optical properties. Bulk absorption is determined by sampling the probability of photon absorption after a path of length  $l$  using an exponential law  $P_{abs}(l) = 1 - e^{-\mu_{abs}(\lambda)l}$ , where  $\mu_{abs}(\lambda)$  is the wavelength-dependent linear absorption coefficient. At the optical boundaries, an analysis is performed depending on the surface type and material properties using Fresnel's equations with polarization dependence [7]. When the film thickness is comparable to the photon wavelength, we use modified Fresnel coefficients to describe the interference effects of optically thin films. The reflection and transmission coefficients are interpreted as probabilities, and therefore the photon is either transmitted or reflected. The simulation outcome is calculated by statistical average of the fate of all histories according to the desired quantity to be evaluated for each experiment. The angular distribution of all photons reflected by the device is constructed in bins with varying resolution to obtain satisfactory statistics per bin.

AB (agb@cdrh.fda.gov) and RJJ are with the Center for Devices and Radiological Health of the U.S. Food and Drug Administration, Rockville, MD. SL and JK are with the Department of Electrical Engineering and Computer Science at the University of Michigan, Ann Arbor, MI. EFK is with the Flat Panel Measurement Laboratory of the National Institute of Standards and Technology, Gaithersburg, MD.

## B. BRDF model

The BRDF, a formalism often used in optics [9], is defined for any reflecting object as the ratio of differential reflected luminance  $dL_o$  to the differential illuminance  $dE_i$  incident on the surface. In this work, we consider the reflectance from the display to be shift-invariant, or independent of position across the screen, therefore neglecting all edge-related phenomena. The complete expression is then given by a six-dimensional function:

$$BRDF(\theta_i, \phi_i, \theta_o, \phi_o, \lambda, p) = \frac{dL_o(\theta_o, \phi_o, \lambda, p)}{dE_i(\theta_i, \phi_i, \lambda, p)} \quad (1)$$

where  $\lambda$  is the photon wavelength and  $p$  is the polarization of the incoming light beam. The BRDF has units of  $sr^{-1}$ . The angle of incidence of ambient light is defined by  $(\theta_i, \phi_i)$ , while  $(\theta_o, \phi_o)$  are the angles that define the direction of reflected light.

The precise evaluation of this function is time consuming and costly. The BRDF can be measured with a goniometric setup with fixed light source and variable detector, with variable source and fixed detector, or with a conoscopic approach where the directional intensity is mapped into a two-dimensional distribution recorded by a position-sensitive planar detector. The first two methods suffer from severe dependence of source and detector positioning precision which has to be less than  $1^\circ$ . The third method requires expensive instrumentation.

The models of display devices presented in this paper are based on uniform slabs representing multiple material layers. In flat panel display devices, the specific details of the pixel structure influence reflection and propagation of light within the different layers. In this model, we incorporate the effect of device features at the pixel level into a general description of the scattering properties at the surface between the pixel circuits and the substrate. With this assumption, the light scattering processes can be considered radially-symmetric,<sup>1</sup> and the BRDF can be described by a function  $B'$  given by

$$B'(\alpha_i, \alpha_o, \lambda, P) = \frac{dL_o(\alpha_o, \lambda, P)}{dE_i(\alpha_i, \lambda, P)} \quad (2)$$

In this study, we consider only the integrated response to an unpolarized light source with flat spectrum in the range from 400 to 800 nm. Therefore, integrating over all  $\lambda$  and  $p$  for a given light source described by  $S(\lambda)$  and  $p$  yields a simplified function

$$B^{\alpha_i}(\alpha_o) = dL_o(\alpha_o)/dE_i(\alpha_i) \quad (3)$$

<sup>1</sup>This assumption is not true for emissive displays with polarizer films or for liquid crystal displays. An extension of this work to include such structures is in progress.

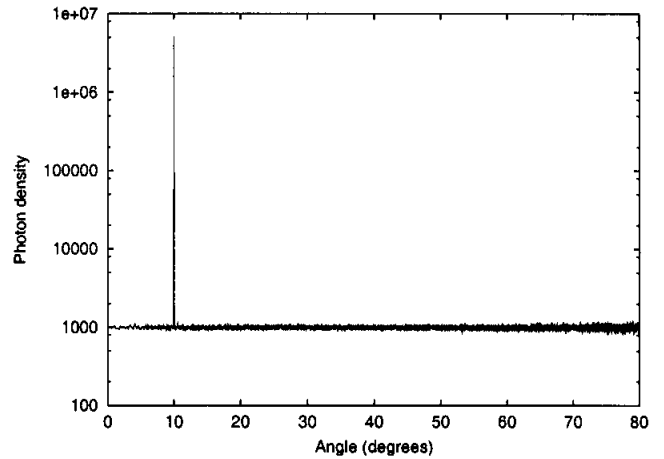


Fig. 1.  $B(\alpha)$  for a surface with 50% specular and 50% diffuse components. The specular fraction results in a delta function at the specular angle of incidence (in this case  $10^\circ$ ). The correction with a factor equal to  $\cos(\alpha)$  yields a horizontal profile, typical of Lambertian surfaces.

Finally, the angular distribution function contained in equally spaced bins from the Monte Carlo simulations is reduced to a luminance distribution density in the range of  $[0, 90^\circ]$  for a given incidence angle  $\alpha_i$  with a factor  $1/\cos(\alpha_o)$ . The introduction of this factor is needed to directly relate the distribution density in angles with the expected angular variations in the luminance out of the device ( $L$ ).  $B^{\alpha_i}(\alpha_o)$  is also known as the in-plane or two-dimensional BRDF. Eq. 4 shows the final metric computed from the Monte Carlo simulations.

$$B^{\alpha_i}(\alpha_o) = \frac{dL(\alpha_o)/\cos(\alpha_o)}{dE(\alpha_i)} \quad (4)$$

Let us consider a reflective surface for which half of the time photons are reflected specularly, and the rest of the time, undergo diffuse reflection according to a Lambertian distribution. For this case, the BRDF is known analytically and is given by Eq. 5, taking into account the number of histories ( $H$ ) and the number of angular bins ( $\beta$ ),

$$B^{\alpha_i}(\alpha_o) = \begin{cases} 0.5H & \alpha_o = \alpha_i, \\ \frac{1}{\beta}(2 \times 0.5 \times H) & \alpha_o \neq \alpha_i. \end{cases} \quad (5)$$

The factor of 2 comes from the summation of photons at positive and negative angles with respect to the surface normal. Fig. 1 shows the output angular distribution  $B^{10}(\alpha_o)$  of an ideal Lambertian surface with a 50% specular component. The expected flat response of a Lambertian surface is seen in the simulation results. For this case, the number of angular bins provides an angular resolution of  $0.009^\circ$  ( $\beta = 10^4$ ), therefore:

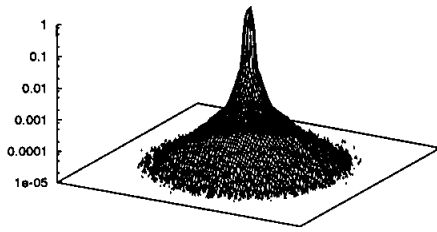


Fig. 2. Detected photon density using a  $100 \times 100$  binning array corresponding to a high resolution monochrome CRT, simulated using a sensor array in close proximity to the display screen.

$$B^{10}(\alpha_o) = \begin{cases} 5 \times 10^6 & \alpha_o = 10^\circ, \\ 10^3 & \alpha_o \neq \alpha_i. \end{cases} \quad (6)$$

The dimensionless specular reflection coefficient  $R_S$  is approximately given by the ratio of the raw specular peak amplitude to the total number of histories:

$$R_S \approx \frac{\text{number of photons in the specular peak}}{\text{total number of photon histories}} \quad (7)$$

which in this case is  $R_S = 0.5$ . Analogously, the diffuse reflection coefficient  $R_D$  (in nit/lux) can be approximated by the ratio of the fraction of non-specular photons over  $2\pi$  to compensate for the emission into the hemisphere:

$$R_D \approx \frac{B^{10}(0)}{\beta} \frac{1}{2\pi} = 0.02 \text{ sr}^{-1} \quad (8)$$

The corresponding detected photon density per pixel using a  $100 \times 100$  binning array at the exit plane is shown in Fig. 2. The in-plane photon density is peaked at the center where the incident beam impinges on the display.

### III. RESULTS

We present results for incident collimated sources at  $10^\circ$ . We used a fixed light source with flat spectral distribution from 400 to 800 nm. For instance, Fig. 1 shows the output angular distribution of an ideal Lambertian diffuser surface with a 50% specular component. It can be shown that the specular reflection coefficient  $R_S$  is approximately given by the ratio of the raw specular peak amplitude to the total number of histories, and that  $R_D$  can be calculated using Eq. 8 [2].

To model typical high-performance medical imaging CRT monitors, we used a structure validated in previous work [3]. The CRT emissive structures consisted of an absorptive glass faceplate of 13 mm with a phosphor layer

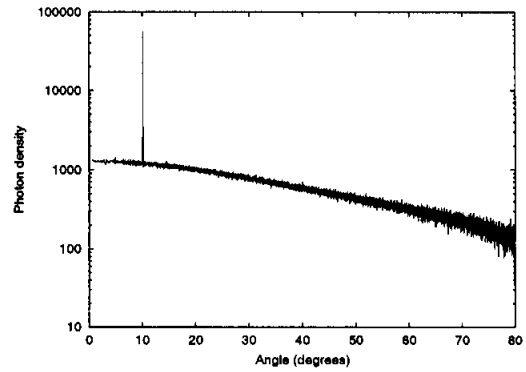


Fig. 3.  $B^{10}(\alpha_o)$  for a monochrome CRT with geometrical and material models described in [1] for an incidence angle of  $10^\circ$  using  $H = 10^6$ .

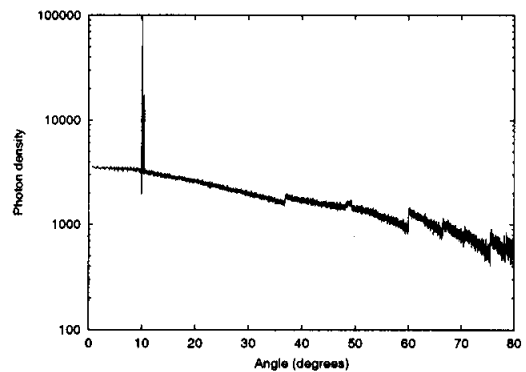


Fig. 4.  $B^{10}(\alpha_o)$  for an OLED device with geometrical and material models described in [4] for an incidence angle of  $10^\circ$  using  $H = 10^6$ .

having a diffuse reflectance of 0.90-0.99, and an anti-reflective coating. Fig. 3 shows the specular and quasi-Lambertian components typical of CRTs. The value of the specular coefficient  $R_S$  calculated from the raw specular peak is around 0.045, and  $R_D$  is around  $0.02 \text{ sr}^{-1}$ . These values agree well with previous measurements of similar devices [1]. The decrease in luminance with angle can be associated with the absorption in the faceplate and most importantly, with the non-Lambertian nature of the reflections. We conclude from these results that the diffuse reflections (and possibly the emissions) from CRTs are more forward-peaked than would be the case for a perfect Lambertian diffuser. These results are consistent with recent observations reported by Blume [6] where the luminance of CRTs was measured at different viewing directions using a spot photometer.

Organic light-emitting displays are simulated using a typical structure model that includes measured optical properties for the organic polymer films and the substrate [4]. The OLED model represents a hetero-structure OLED described by He *et al.* [10] with an aluminum cathode electrode and a transparent anode ITO electrode (160

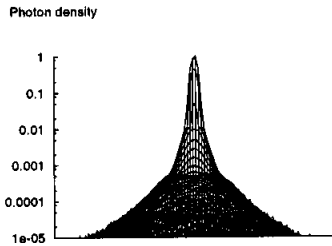


Fig. 5. Normalized reflected spot profile for the CRT model.

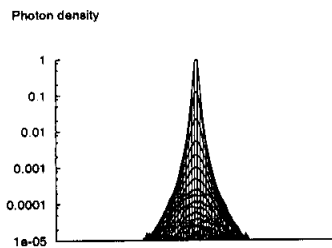


Fig. 6. Normalized reflected spot profile for the OLED model.

nm, refractive index 1.8). The organic polymer film thickness used was 200 nm. The substrate index of refraction was 1.5 and its thickness 900  $\mu\text{m}$ . Fig. 4 shows  $B^{10}(\alpha_o)$  for OLEDs. It can be observed that the specular component is predominant ( $R_S = 0.10$ ,  $R_D = 0.06 \text{ sr}^{-1}$ ). The results reveal that the specular peak has a significant width. This observation is consistent with an intermediate component of reflection observed in flat-panel displays or haze, caused by local light scattering. The spread of the specular peak shows the difficulty in defining specifically the specular and haze regions. We note that the diffuse component follows a quasi-Lambertian profile with about the same fall-off rate with off-axis angle found for the CRT models. We speculate that the several discontinuities are associated with refractive index changes of the different layers of the OLED stack. From the simulation results, it is possible to compute a haze ratio associated with the full width at half maximum of about  $2^\circ$ . However, as described in experimental studies, the value of the haze ratio is very sensitive to the cut-off limit. In Figs. 5 and 6, we show a comparison of the simulated reflected beam spot profiles for the CRT and OLED model. The significant diffuse reflections off the CRT phosphor layer cause blur. For the OLED model, the mirror-like appearance of the reflected spot is consistent with a small diffuse component.

#### IV. DISCUSSION

We present a novel method based on Monte Carlo techniques to calculate the bidirectional reflectance distribution function of emissive displays. We demonstrate the validity of the results using simple models for which the exact analytical solution is known, and by comparing the results with experimental measurements. We conclude that for both emissive display technologies, the reflections are slightly more forward-peaked than the predictions of Lambertian profiles. We show that the BRDF of OLED displays based on polymer films backed with a metallic reflective electrode is highly specular. We report for the first time the complete BRDF signature of OLEDs, showing that the haze component is small, with a characteristic width of  $2^\circ$ . This intermediate component of reflection complicates the measurement of the specular peak since luminance meters having slightly different apertures will produce a specular reflection component with large errors. This modelling tool will be used to demonstrate improvements of novel designs for achieving high-contrast in high-illuminance environments without the need to fabricate test devices, or use expensive instrumentation. We are investigating the effect of the optical properties and absorptive layers on the reflectance properties of OLEDs, and the BRDF signatures of liquid crystal displays.

#### REFERENCES

- [1] A. Badano. *Image Quality Degradation by Light Scattering Processes in High Performance Display Devices for Medical Imaging*. PhD thesis, University of Michigan, 1999.
- [2] A. Badano. Monte Carlo modeling of the bidirectional reflectance of display devices. *In preparation*, 2001.
- [3] A. Badano, M. J. Flynn, E. Muka, K. Compton, and T. Monsees. The veiling glare point-spread function of medical imaging monitors. In *Proceedings of the SPIE Medical Imaging Display Conference*, 1999.
- [4] A. Badano and J. Kanicki. Monte carlo analysis of the spectral photon emission and extraction efficiency of organic light-emitting devices. *Journal of Applied Physics*, 90(4), 2001.
- [5] M. E. Becker. Evaluation and characterization of display reflectance. *Displays*, 19:35–54, 1998.
- [6] H. Blume. In *Proceedings of the SPIE Medical Imaging Conference*, volume 4323-07, 2001.
- [7] M. Born and E. Wolf. *Principles of Optics*. 3rd revised edition, 1965.
- [8] J. Delacour, S. Ungar, G. Mathieu, G. Hasna, P. Martinez, and J.-C. Roche. Front panel engineering with CAD simulation tool. In *Proceedings of the SPIE Flat Panel Display Technology and Display Metrology Conference*, 1999.
- [9] M. Elias, L. Simonot, and M. Menu. Bidirectional reflectance of a diffuse background covered by a partly absorbing layer. *Optics Communications*, 191:1–7, 2001.
- [10] Y. He, S. Gong, R. Hattori, and J. Kanicki. *Applied Physics Letters*, 74, 1999.
- [11] E. F. Kelley. Display reflectance model based on BRDF. *Displays*, 19:27–34, 1998.